

# Beyond the spontaneous scalarization: New fully nonlinear dynamical mechanism for formation of scalarized black holes

Daniela D. Doneva<sup>1,2,\*</sup> and Stoytcho S. Yazadjiev<sup>1,3,4,†</sup>

<sup>1</sup>*Theoretical Astrophysics, Eberhard Karls University of Tübingen, Tübingen 72076, Germany*

<sup>2</sup>*INRNE - Bulgarian Academy of Sciences, 1784 Sofia, Bulgaria*

<sup>3</sup>*Department of Theoretical Physics, Faculty of Physics, Sofia University, Sofia 1164, Bulgaria*

<sup>4</sup>*Institute of Mathematics and Informatics, Bulgarian Academy of Sciences, Acad. G. Bonchev St. 8, Sofia 1113, Bulgaria*

In the present paper we show the existence of a fully nonlinear dynamical mechanism for the formation of scalarized black holes which is different from the spontaneous scalarization. We consider a class of scalar-Gauss-Bonnet gravity theories within which no tachyonic instability can occur. Although the Schwarzschild black holes are linearly stable against scalar perturbations, we show dynamically that for certain choices of the coupling function they are unstable against nonlinear scalar perturbations. This nonlinear instability leads to the formation of new black holes with scalar hair. The fully nonlinear and self-consistent study of the equilibrium black holes reveals that the spectrum of solutions is more complicated possessing additional branches with scalar field that turn out to be unstable, though. The formation of scalar hair of the Schwarzschild black hole will always happen with a jump because the stable “scalarized branch” is not continuously connected to Schwarzschild one.

## I. INTRODUCTION

Spontaneous scalarization is a dynamical mechanism for endowing black holes (and other compact objects) with scalar hair without altering the predictions in the weak field limit [1–5]. It is a strong gravity phase transition triggered by tachyonic instability due to the non-minimal coupling between the scalar field(s) and the spacetime curvature (or matter). The realistic black hole spontaneous scalarization was mainly studied within the scalar-Gauss-Bonnet (sGB) gravity defined by the action

$$S = \frac{1}{16\pi} \int d^4x \sqrt{-g} \left[ R - 2\nabla_\mu \phi \nabla^\mu \phi + \lambda^2 f(\phi) \mathcal{R}_{GB}^2 \right] \quad (1)$$

where  $R$  is the Ricci scalar with respect to the spacetime metric  $g_{\mu\nu}$ ,  $\phi$  denotes the scalar field with a coupling function  $f(\phi)$ ,  $\lambda$  is the so-called Gauss-Bonnet coupling constant having dimension of *length* and  $\mathcal{R}_{GB}^2 = R^2 - 4R_{\mu\nu}R^{\mu\nu} + R_{\mu\nu\alpha\beta}R^{\mu\nu\alpha\beta}$  is the Gauss-Bonnet invariant with  $R_{\mu\nu\alpha\beta}$  being the curvature tensor. Black hole spontaneous scalarization was extensively studied (see e.g. [3–11]), including the rotating case [12, 13] and the spin-induced scalarization [14–18]. It turn out that these black holes are energetically favorable over the GR solutions and they are stable [19–21]. The nonlinear dynamics of scalarized black holes in sGB gravity, including mergers and stellar core-collapse, was examined in

[22–26]. Spontaneous scalarization was also considered in other alternative theories of gravity [27–32].

In the present work we would like to go beyond the spontaneous scalarization. We pose the following problem. Let us consider sGB theories with coupling functions that do not allow for a tachyonic instability to occurs, i.e. sGB theories which do not exhibit spontaneous scalarization. Then we ask: Is there another dynamical mechanism for producing scalar hair of the black holes? The purpose of this paper is to answer this question.

We identify a class of sGB theories with coupling between the scalar field and the Gauss-Bonnet invariant that *can not exhibit* spontaneous scalarization for black holes but admits all of the stationary solutions of general relativity, including the Schwarzschild black holes. Within the mentioned class of sGB theories the Schwarzschild black holes are linearly stable. However, we show dynamically that they are unstable against nonlinear scalar perturbations within the sGB gravity and that the nonlinear instability leads to the formation of new black holes with scalar hair.

In Sec. II we discuss the nonlinear instability of the Schwarzschild black hole in the mentioned class of sGB gravity and the dynamical formation of scalarized black holes for a certain Gauss-Bonnet coupling function. The results for the equilibrium scalarized black hole branches are presented in Sec. III. The paper ends with conclusions. In the appendixes we present the necessary mathematical background as well as our results for a second Gauss-Bonnet coupling function.

\* daniela.doneva@uni-tuebingen.de

† yazad@phys.uni-sofia.bg

## II. NONLINEAR INSTABILITY OF THE SCHWARZSCHILD BLACK HOLE AND DYNAMICAL FORMATION OF SCALARIZED BLACK HOLES

As discussed above we consider sGB theories which can not exhibit tachyonic instability. Therefore we impose the following conditions on the Gauss-Bonnet coupling function

$$f(0) = 0, \quad \frac{df}{d\varphi}(0) = 0, \quad \frac{d^2f}{d\varphi^2}(0) = 0. \quad (2)$$

The first condition can always be imposed since the field equations include only the first derivative of the coupling function but not the coupling function itself. The second condition guarantees the Schwarzschild solution is also a black hole solution to the equations of the sGB gravity with  $\varphi = 0$ . It is no difficult one to see that the third condition  $\frac{d^2f}{d\varphi^2}(0) = 0$  imposed on the Gauss-Bonnet coupling function leads to the fact that no tachyonic instability is possible – the Schwarzschild solution is stable against linear scalar perturbations. Indeed, in the case of  $\frac{d^2f}{d\varphi^2}(0) = 0$  the equation governing the scalar perturbations is just the scalar wave equation and it is a well-known fact the Schwarzschild black hole is stable against the linear perturbations of a massless scalar perturbations. Therefore, if black holes with scalar hair exist, they should form a new black hole phase coexisting with the usual Schwarzschild black hole phase. It will be called a scalarized black hole phase.

We will investigate how the scalarized phases of the Schwarzschild black hole can be dynamically formed and whether they are stable. Since the full nonlinear dynamics of black holes in sGB gravity is a complicated task, we shall base our study on an approximate model which is free from heavy technical complications but preserves the leading role of the nonlinearity associated with the coupling function. More precisely, we shall consider a model where the spacetime geometry is kept fixed and the whole dynamics is governed by the nonlinear equation for the scalar field. This dynamical model is a very good approximation for example when the energy of the scalar hair is less than the full mass of the black hole [24]. Technically speaking, we will consider the nonlinear wave equation (A2) on the Schwarzschild background geometry with the requirements that the scalar field perturbation has the form of an outgoing wave at infinity and an ingoing wave at the black hole horizon. We will follow closely the methodology described in [15, 24].

The conditions for the existence of scalarized phases (2) is easily satisfied by a coupling function containing power of  $\varphi$  higher than two. In the present paper we

are focusing on  $Z_2$  symmetric theories and the first two possible choices are  $\varphi^4$  and  $\varphi^6$ . In the case when the coupling functions are directly proportional to  $\varphi^4$  and  $\varphi^6$ , though, we could not find any stable solutions. This observation is similar to the case of standard scalarization in sGB theories where different ways to “stabilize” the scalarized black hole solutions were proposed [6–9]. Perhaps the most straightforward and easy to handle from a numerical point of view is to consider an exponential coupling function. In our numerical simulations we consider two forms of the coupling function:

$$f_1(\varphi) = \frac{1}{4\beta} (1 - e^{-\beta\varphi^4}), \quad f_2(\varphi) = \frac{1}{6\beta} (1 - e^{-\beta\varphi^6}) \quad (3)$$

where  $\beta$  is a parameter. Both of them fulfill the conditions (2). In the main text we present our results for the coupling function  $f_1(\varphi)$  while the results for the coupling function  $f_2(\varphi)$  are given in Appendix B.

For these choices of the coupling function, the Schwarzschild black hole is stable only with respect to linear perturbations and it might be unstable with respect to larger nonlinear perturbations. By evolving in time the nonlinear scalar field equation (A6) on the Schwarzschild background (i.e. consider the time evolution of the system in the decoupling limit approximation), it turns out that there is a threshold amplitude of the perturbation above which the Schwarzschild black hole loses stability and a scalarized phase forms. This is demonstrated in Fig. 1 where the time evolution of the scalar field on the Schwarzschild background is shown for several amplitudes of the initial perturbation. As one can see, for small amplitudes the standard quasinormal modes and exponential decay is observed. Once the amplitude exceed a certain threshold, the scalar field stabilizes to a constant at late times that is exactly the formation of a scalarized phase. It is important to note, that through this approach only the formation of a stable scalarized phase can be observed. As we will see later, more than one scalarized phase can exist that can be constructed by solving the static field equations. Independent on the initial data, though, we have always seen the formation of solutions belonging to only one of the branches that is a strong indication that it is the only stable one. In order to prove rigorously the stability of a scalarized phase one should consider the coupled system of equations of the metric and the scalar field, i.e. to drop the decoupling limit approximation. Our experience shows, though, that considering only the scalar field evolution often gives correct results for the stability/instability of scalarized black holes [24].

The method described above can give us very important intuition where stable scalarized phases can exist

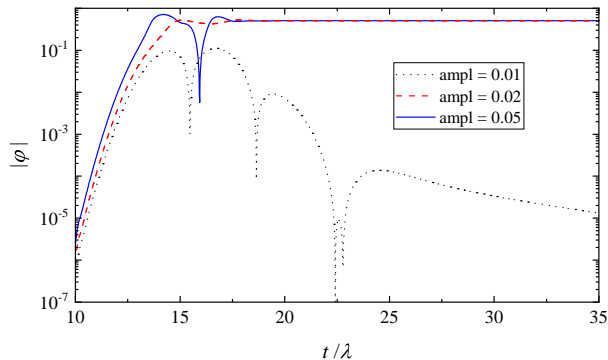


FIG. 1. The time evolution of the scalar field on the background of a Schwarzschild black hole with mass  $M/\lambda = 0.1$  and  $\beta = 50$ . The initial data is a Gauss pulse with amplitudes 0.001, 0.002 and 0.005, dispersion  $\sigma/\lambda = 1$ , located at coordinate distance  $x/\lambda = 12$ . The coupling function is  $f_1(\varphi)$ .

and how they form dynamically. In order to study the full spectrum of solution, including the unstable ones, and their domain of existence taking into account the regularity condition (A15), one has to solve the fully nonlinear and self-consistent system of reduced field equations in the case of static and spherically symmetric spacetime [3]. The results are presented in the next section.

### III. SCALARIZED PHASES

We study in detail the spectrum of solutions describing scalarized phases of the Schwarzschild black hole by solving the fully nonlinear and self-consistent system of reduced field equations (A8)–(A11) with the appropriate boundary conditions. The solutions will be calculated numerically using a methodology similar to [3]. All the results in this sections are for the Gauss-Bonnet coupling function  $f_1(\varphi)$ .

The scalarized phases of the Schwarzschild black hole are displayed in Figs. 2 and 3 where the scalar field on the horizon, the mass and the scalar charge are given for several values of  $\beta$ . Here the scalar charge  $D$  is defined as the coefficient in the leading order asymptotic of the scalar field at infinity

$$\varphi|_{r \rightarrow \infty} \sim \frac{D}{r}. \quad (4)$$

All dimensional quantities are normalized with respect to  $\lambda$ . Only the solutions with  $\varphi > 0$  are displayed but one should keep in mind that the field equations, with this choice of the coupling function (3), are symmetric with respect to a change of the sign of  $\varphi$  and thus the

solutions with the same metric functions but opposite sign of  $\varphi$  also exist.

Several branches of hairy black holes can exist and the qualitative picture is different for different  $\beta$ . The three possible cases with proper choices of  $\beta$  are shown separately in Fig. 2:

- For large enough  $\beta$  (bottom panel) two branches of solutions exist and both of them start from the  $M = 0$  limit. One of the branches has vanishing scalar field at the horizon for  $M \rightarrow 0$ , while the scalar field for the other seems to increase as  $M$  approaches zero. According to the results from the nonlinear evolution of the scalar field, the latter branch (depicted with solid line) is the only stable one.
- For intermediate  $\beta$  (middle panel) up to three branches can exist. The lower one (dotted line) having  $\varphi_H \rightarrow 0$  when  $M \rightarrow 0$  is terminated at some finite  $M/\lambda$  where the solutions disappear due to violation of the regularity condition (A15). The upper branch (solid line) starts from zero mass and with the increase of  $M/\lambda$  the scalar field on the horizon decreases until a minimum of  $M/\lambda$  is reached. At that point the branch merges with a third middle branch of solutions (dashed line). This middle branch is also terminated at a finite  $M/\lambda$ . According to the results from the nonlinear evolution of the scalar field, the uppermost branch (depicted with solid line) is the only stable one.
- For small  $\beta$  (upper panel) there are also three branches of solutions but the upper two merge at two points – at their beginning and at the end of the branch. Again, the stable branch is the one depicted with solid line.

This picture is clearly different from the Einstein-Maxwell-scalar gravity [33] where up to two scalarized branches exist and one of them originates from the extremal Reissner-Nordström solution. Here clearly no extremal solution exists. Instead, most probably the solutions are connected with a solitonic-like solutions in sGB gravity of the type considered in [34, 35].

The change of the branches as  $\beta$  is varied can be better observed in the top panel of Fig. 3. In this figure there is a clustering of the lower mass black hole branches for different  $\beta$  depicted with dotted line (the area shaded in gray in the figure), but the rest of the branches can be well resolved. As one can see, with the decrease of  $\beta$  the larger mass branch depicted with solid line, that is actually the stable one, gets shorter until it completely disappears that happens for roughly  $\beta \approx 20$ . On the

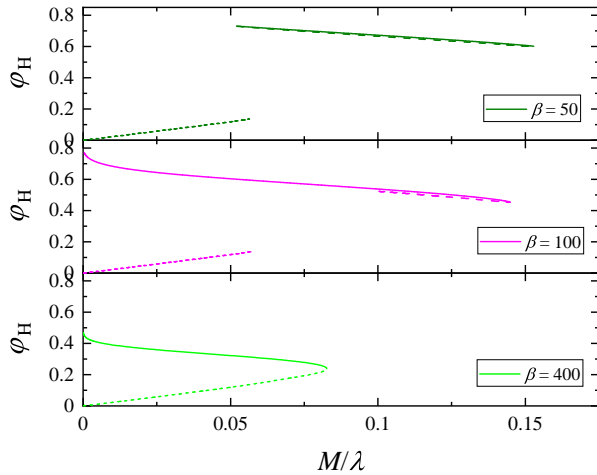


FIG. 2. The scalar field at the horizon as a function of mass for tree value of  $\beta$  demonstrating the tree possible configurations of scalarized phase branches discussed in the text.

contrary, we could not find an upper limit on  $\beta$  for the existence of scalarized phases. The branches, though, span a smaller range of masses with the increase of  $\beta$ .

The radius of the horizon can differ significantly from the Schwarzschild one especially for small  $\beta$  and gets closer to GR with the increase of  $\beta$ . This behavior is similar to the standard scalarization [36] where also the differences from the Schwarzschild black hole are reduced for larger  $\beta$ .

As one can see in the top and middle panels of Fig. 3 the differences especially between the two upper branches (for a fixed  $\beta$ ) are very small and seem negligible. We have performed, though, extensive numerical experiments to confirm that indeed these solutions exist and they are not a numerical artifact. If one looks at the scalar charge, that is plotted in the lower panel, then a clear difference between the branches is observed. Thus, even though at the black hole horizon their properties are quite similar, the overall scalar field profile and asymptotic are quite distinct.

Having discussed the properties of the scalarized phases, the next step is to determine which are the stable branches (apart from the Schwarzschild solution that is always linearly stable for the coupling (3)). We already had an indication from the evolution of the scalar field that only the branch depicted with solid line in Figs. 2 and 3 is stable. Here we will take a different approach by looking at the thermodynamical properties of these black holes. We can define the entropy at the horizon in the following way [3]

$$S_H = \frac{1}{4}A_H + 4\pi\lambda^2 f(\varphi_H). \quad (5)$$

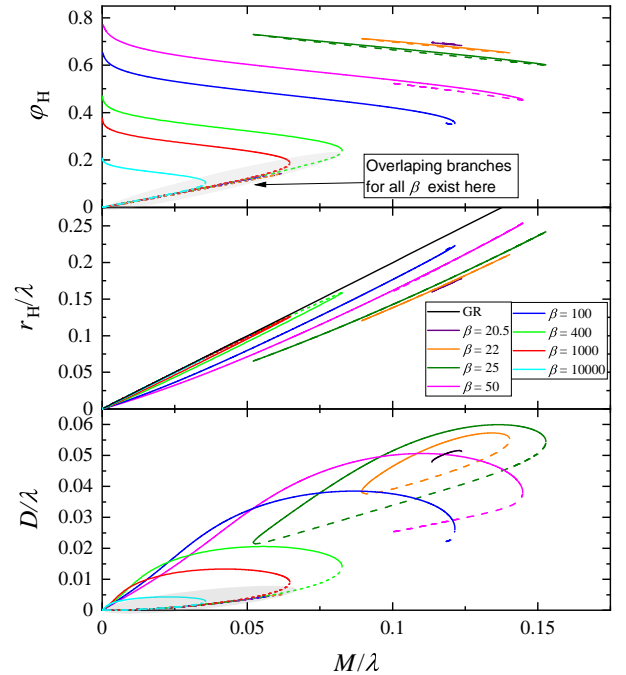


FIG. 3. The scalar field at the horizon (top panel), the mass (middle panel) and the scalar charge (bottom panel) as functions of the black hole horizon mass for the  $f_1(\varphi)$  coupling.

The black hole entropy as a function of mass is plotted in Fig. 4 for all of the branches and values of  $\beta$ . Something important that might be a bit hard to notice in this scale is that among the scalarized phases (for fixed  $\beta$ ), the one depicted with solid line has the largest entropy and hence it is probably the only stable one. This potentially stable scalarized phase, though, does not always have larger entropy compared to the Schwarzschild one. For larger  $\beta$  the following behavior is typical. For larger black hole masses the entropy is smaller making the Schwarzschild black hole the thermodynamically preferred one while there is a transition point at smaller masses, below which the scalarized phase acquires the larger entropy. Interestingly, the behavior changes in the small  $\beta$  regime where the whole scalarized phase branch has larger entropy compared to the Schwarzschild one and is thus thermodynamically preferred.

the

#### IV. CONCLUSION

In the present paper we have considered the possibilities to go beyond the standard scalarization of black holes in scalar-Gauss-Bonnet gravity. We showed the existence of a fully nonlinear dynamical mechanism for the formation of scalarized black holes which

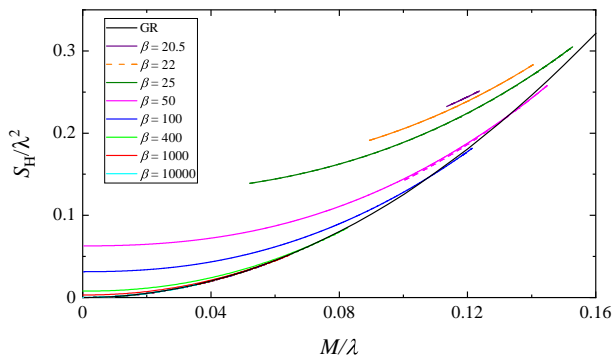


FIG. 4. The entropy at the black hole horizon as a function of the black hole mass for the  $f_1(\varphi)$  coupling.

is different from the spontaneous scalarization. We considered types of coupling functions for which the Schwarzschild black hole is still a linearly stable solution of the field equations but for certain ranges of the parameters scalarized phases of the Schwarzschild black hole can exist. The reason for the appearance of such phases is that even though the Schwarzschild phase is stable against small (linear) perturbations, this stability can be lost for larger amplitudes of the perturbations that will bring us in the nonlinear regime. We demonstrate this explicitly by evolving the nonlinear scalar field equation in sGB gravity on the Schwarzschild background and observe that indeed a nontrivial scalar field can develop for certain ranges of the parameters if the amplitude of the perturbations is large enough. The obtained in this way scalarized phases are not continuously connected to the Schwarzschild black hole, i.e. they do not bifurcate from it unlike the case of standard scalarization, and they are most probably stable.

Even though the time evolution method can demonstrate the formation of scalarized phases, it can not be used to obtain the full spectrum of hairy solutions, including the unstable ones. For this purpose we solved the reduced system of field equations in the case of static and spherically symmetric spacetime and scalar field configurations. We have found that up to three branches of scalarized phases can exist that have a complicated structure depending on the parameter  $\beta$  in the coupling functions (3). A common feature is that a minimum  $\beta$  exists below which no scalarized phases are present, while such hairy solutions can be found for arbitrary larger  $\beta$

but the range of black hole masses where they exist is decreased.

As expected, the stable scalarized phase has the largest entropy among all the branches of hairy black holes. For larger  $\beta$  and close to the maximum mass of the corresponding branch, the stable scalarized phase can have smaller entropy than the Schwarzschild black hole making it thermodynamically less favorable. This quickly changes with the decrease of the mass and for smaller masses the scalarized phase has larger entropy. For smaller  $\beta$  the scalarized phase is always thermodynamically favorable over the Schwarzschild phase.

As we commented, the stable scalarized phase is not continuously connected to the Schwarzschild one but instead there is a (sometimes large) “gap” between the two. This can have serious astrophysical implications because the transition from one phase to the other will happen with a jump contrary to the standard scalarization where the transition from non-scalarized to scalarized state can be continuous. In the present paper we have examined how large scalar field perturbations excite the scalar field but it will be extremely interesting to understand whether and how perturbations of the metric can excite the scalarized phase. This will have direct application to astrophysical processes such as black hole mergers. In order to do this one has to drop the decoupling limit approximation and consider the full dynamics of the system that is a study underway.

In a forthcoming paper we will show that the discussed nonlinear mechanism for formation of black holes with scalar hair works also for rotating black holes. Within the considered class of sGB theories (with coupling functions of the form  $f_1(\varphi)$  and  $f_2(\varphi)$ ) the Kerr solution is linearly stable but suffers from nonlinear instability within sGB gravity and this nonlinear instability gives rise to new rotating scalarized black holes.

## ACKNOWLEDGEMENTS

DD acknowledges financial support via an Emmy Noether Research Group funded by the German Research Foundation (DFG) under grant no. DO 1771/1-1. SY would like to thank the University of Tuebingen for the financial support. The partial support by the Bulgarian NSF Grant KP-06-H28/7 and the Networking support by the COST Actions CA16104 and CA16214 are also gratefully acknowledged.

[1] T. Damour and G. Esposito-Farese, *Physical Review Letters* **70**, 2220 (1993).

[2] T. Damour and G. Esposito-Farèse, *Phys. Rev. D* **54**, 1474 (1996).

- [3] D. D. Doneva and S. S. Yazadjiev, Phys. Rev. Lett. **120**, 131103 (2018), arXiv:1711.01187 [gr-qc].
- [4] H. O. Silva, J. Sakstein, L. Gualtieri, T. P. Sotiriou, and E. Berti, Phys. Rev. Lett. **120**, 131104 (2018), arXiv:1711.02080 [gr-qc].
- [5] G. Antoniou, A. Bakopoulos, and P. Kanti, Phys. Rev. Lett. **120**, 131102 (2018), arXiv:1711.03390 [hep-th].
- [6] M. Minamitsuji and T. Ikeda, Phys. Rev. D **99**, 044017 (2019), arXiv:1812.03551 [gr-qc].
- [7] H. O. Silva, C. F. Macedo, T. P. Sotiriou, L. Gualtieri, J. Sakstein, and E. Berti, Phys. Rev. D **99**, 064011 (2019), arXiv:1812.05590 [gr-qc].
- [8] D. D. Doneva, K. V. Staykov, and S. S. Yazadjiev, Phys. Rev. D **99**, 104045 (2019), arXiv:1903.08119 [gr-qc].
- [9] C. F. B. Macedo, J. Sakstein, E. Berti, L. Gualtieri, H. O. Silva, and T. P. Sotiriou, Phys. Rev. D **99**, 104041 (2019), arXiv:1903.06784 [gr-qc].
- [10] J. L. Blázquez-Salcedo, B. Kleihaus, and J. Kunz (2021) arXiv:2106.15574 [gr-qc].
- [11] G. Antoniou, A. Lehébel, G. Ventagli, and T. P. Sotiriou, (2021), arXiv:2105.04479 [gr-qc].
- [12] P. V. Cunha, C. A. Herdeiro, and E. Radu, Phys. Rev. Lett. **123**, 011101 (2019), arXiv:1904.09997 [gr-qc].
- [13] L. G. Collodel, B. Kleihaus, J. Kunz, and E. Berti, Class. Quant. Grav. **37**, 075018 (2020), arXiv:1912.05382 [gr-qc].
- [14] A. Dima, E. Barausse, N. Franchini, and T. P. Sotiriou, Phys. Rev. Lett. **125**, 231101 (2020), arXiv:2006.03095 [gr-qc].
- [15] D. D. Doneva, L. G. Collodel, C. J. Krüger, and S. S. Yazadjiev, Phys. Rev. D **102**, 104027 (2020), arXiv:2008.07391 [gr-qc].
- [16] D. D. Doneva, L. G. Collodel, C. J. Krüger, and S. S. Yazadjiev, (2020), arXiv:2009.03774 [gr-qc].
- [17] C. A. Herdeiro, E. Radu, H. O. Silva, T. P. Sotiriou, and N. Yunes, (2020), arXiv:2009.03904 [gr-qc].
- [18] E. Berti, L. G. Collodel, B. Kleihaus, and J. Kunz, (2020), arXiv:2009.03905 [gr-qc].
- [19] J. L. Blázquez-Salcedo, D. D. Doneva, J. Kunz, and S. S. Yazadjiev, Phys. Rev. D **98**, 084011 (2018), arXiv:1805.05755 [gr-qc].
- [20] J. L. Blázquez-Salcedo, D. D. Doneva, S. Kahlen, J. Kunz, P. Nedkova, and S. S. Yazadjiev, Phys. Rev. D **101**, 104006 (2020), arXiv:2003.02862 [gr-qc].
- [21] J. L. Blázquez-Salcedo, D. D. Doneva, S. Kahlen, J. Kunz, P. Nedkova, and S. S. Yazadjiev, Phys. Rev. D **102**, 024086 (2020), arXiv:2006.06006 [gr-qc].
- [22] J. L. Ripley and F. Pretorius, Class. Quant. Grav. **37**, 155003 (2020), arXiv:2005.05417 [gr-qc].
- [23] H. O. Silva, H. Witek, M. Elley, and N. Yunes, (2020), arXiv:2012.10436 [gr-qc].
- [24] D. D. Doneva and S. S. Yazadjiev, Phys. Rev. D **103**, 064024 (2021), arXiv:2101.03514 [gr-qc].
- [25] H.-J. Kuan, D. D. Doneva, and S. S. Yazadjiev, (2021), arXiv:2103.11999 [gr-qc].
- [26] W. E. East and J. L. Ripley, (2021), arXiv:2105.08571 [gr-qc].
- [27] C. A. Herdeiro, E. Radu, N. Sanchis-Gual, and J. A. Font, Phys. Rev. Lett. **121**, 101102 (2018), arXiv:1806.05190 [gr-qc].
- [28] N. Andreou, N. Franchini, G. Ventagli, and T. P. Sotiriou, Phys. Rev. D **99**, 124022 (2019), [Erratum: Phys. Rev. D **101**, 109903 (2020)], arXiv:1904.06365 [gr-qc].
- [29] Y.-X. Gao, Y. Huang, and D.-J. Liu, Phys. Rev. D **99**, 044020 (2019), arXiv:1808.01433 [gr-qc].
- [30] D. D. Doneva and S. S. Yazadjiev, Phys. Rev. D **103**, 083007 (2021), arXiv:2102.03940 [gr-qc].
- [31] S.-J. Zhang, Eur. Phys. J. C **81**, 441 (2021), arXiv:2102.10479 [gr-qc].
- [32] Y. S. Myung and D.-C. Zou, (2021), arXiv:2103.01389 [gr-qc].
- [33] J. L. Blázquez-Salcedo, C. A. R. Herdeiro, J. Kunz, A. M. Pombo, and E. Radu, Phys. Lett. B **806**, 135493 (2020), arXiv:2002.00963 [gr-qc].
- [34] B. Kleihaus, J. Kunz, and P. Kanti, Phys. Lett. B **804**, 135401 (2020), arXiv:1910.02121 [gr-qc].
- [35] B. Kleihaus, J. Kunz, and P. Kanti, Phys. Rev. D **102**, 024070 (2020), arXiv:2005.07650 [gr-qc].
- [36] D. D. Doneva, S. Kiorpelidi, P. G. Nedkova, E. Papantonopoulos, and S. S. Yazadjiev, Phys. Rev. D **98**, 104056 (2018), arXiv:1809.00844 [gr-qc].

## Appendix A: Basic mathematical equations

The variation of action (1) with respect to the metric  $g_{\mu\nu}$  and scalar field  $\varphi$  gives the following field equations

$$R_{\mu\nu} - \frac{1}{2}Rg_{\mu\nu} + \Gamma_{\mu\nu} = 2\nabla_\mu\varphi\nabla_\nu\varphi - g_{\mu\nu}\nabla_\alpha\varphi\nabla^\alpha\varphi \quad (A1)$$

$$\nabla_\alpha\nabla^\alpha\varphi = -\frac{\lambda^2}{4}\frac{df(\varphi)}{d\varphi}\mathcal{R}_{GB}^2, \quad (A2)$$

where  $\nabla_\mu$  is the covariant derivative with respect to  $g_{\mu\nu}$  and  $\Gamma_{\mu\nu}$  is defined by

$$\begin{aligned} \Gamma_{\mu\nu} = & -R(\nabla_\mu\Psi_\nu + \nabla_\nu\Psi_\mu) - 4\nabla^\alpha\Psi_\alpha\left(R_{\mu\nu} - \frac{1}{2}Rg_{\mu\nu}\right) \\ & + 4R_{\mu\alpha}\nabla^\alpha\Psi_\nu + 4R_{\nu\alpha}\nabla^\alpha\Psi_\mu \\ & - 4g_{\mu\nu}R^{\alpha\beta}\nabla_\alpha\Psi_\beta + 4R_{\mu\alpha\nu}^\beta\nabla^\alpha\Psi_\beta \end{aligned} \quad (A3)$$

with

$$\Psi_\mu = \lambda^2\frac{df(\varphi)}{d\varphi}\nabla_\mu\varphi. \quad (A4)$$

### 1. Dynamics

In the decoupling limit we solve eq. (A2) on the Schwarzschild background which in the standard coordinate reads



$$ds^2 = -\frac{\Delta}{r^2} dt^2 + \frac{r^2}{\Delta} dr^2 + r^2(d\theta^2 + \sin^2\theta d\phi^2), \quad (\text{A5})$$

where  $\Delta = r^2 - 2Mr$ . It is convenient to introduce the coordinate  $x$  defined by  $dx = \frac{r^2}{\Delta} dr$ . In the coordinates  $(t, x, \theta, \phi)$  equation eq. (A2) takes the following explicit form

$$-\partial_t^2 \varphi + \partial_x^2 \varphi + \frac{2\Lambda}{r^3} \partial_x \delta \varphi + \frac{\Lambda}{r^4} \left[ \frac{1}{\sin\theta} \partial_\theta (\sin\theta \partial_\theta \varphi) + \frac{1}{\sin^2\theta} \partial_\phi^2 \varphi \right] = -\lambda^2 \frac{12M^2 \Delta}{r^8} \frac{df(\varphi)}{d\varphi}. \quad (\text{A6})$$

The boundary conditions we have to impose when evolving in time eq. (A6) is that the scalar field has the form of an outgoing wave at infinity and an ingoing wave at the black hole horizon

## 2. Static and spherically symmetric equations

We consider further static and spherically symmetric spacetimes as well as static and spherically symmetric scalar field configurations. The spacetime metric can be written then as

$$ds^2 = -e^{2\Phi(r)} dt^2 + e^{2\Lambda(r)} dr^2 + r^2(d\theta^2 + \sin^2\theta d\phi^2) \quad (\text{A7})$$

After using this form of the metric a system of reduced field equations can be derived that describes the static black hole solutions in sGB gravity

$$\frac{2}{r} \left[ 1 + \frac{2}{r} (1 - 3e^{-2\Lambda}) \Psi_r \right] \frac{d\Lambda}{dr} + \frac{(e^{2\Lambda} - 1)}{r^2} - \frac{4}{r^2} (1 - e^{-2\Lambda}) \frac{d\Psi_r}{dr} - \left( \frac{d\varphi}{dr} \right)^2 = 0, \quad (\text{A8})$$

$$\frac{2}{r} \left[ 1 + \frac{2}{r} (1 - 3e^{-2\Lambda}) \Psi_r \right] \frac{d\Phi}{dr} - \frac{(e^{2\Lambda} - 1)}{r^2} - \left( \frac{d\varphi}{dr} \right)^2 = 0, \quad (\text{A9})$$

$$\begin{aligned} & \frac{d^2\Phi}{dr^2} + \left( \frac{d\Phi}{dr} + \frac{1}{r} \right) \left( \frac{d\Phi}{dr} - \frac{d\Lambda}{dr} \right) \\ & + \frac{4e^{-2\Lambda}}{r} \left[ 3 \frac{d\Phi}{dr} \frac{d\Lambda}{dr} - \frac{d^2\Phi}{dr^2} - \left( \frac{d\Phi}{dr} \right)^2 \right] \Psi_r \\ & - \frac{4e^{-2\Lambda}}{r} \frac{d\Phi}{dr} \frac{d\Psi_r}{dr} + \left( \frac{d\varphi}{dr} \right)^2 = 0, \end{aligned} \quad (\text{A10})$$

$$\begin{aligned} & \frac{d^2\varphi}{dr^2} + \left( \frac{d\Phi}{dr} - \frac{d\Lambda}{dr} + \frac{2}{r} \right) \frac{d\varphi}{dr} \\ & - \frac{2\lambda^2}{r^2} \frac{df(\varphi)}{d\varphi} \left\{ (1 - e^{-2\Lambda}) \left[ \frac{d^2\Phi}{dr^2} + \frac{d\Phi}{dr} \left( \frac{d\Phi}{dr} - \frac{d\Lambda}{dr} \right) \right] \right. \\ & \left. + 2e^{-2\Lambda} \frac{d\Phi}{dr} \frac{d\Lambda}{dr} \right\} = 0, \end{aligned} \quad (\text{A11})$$

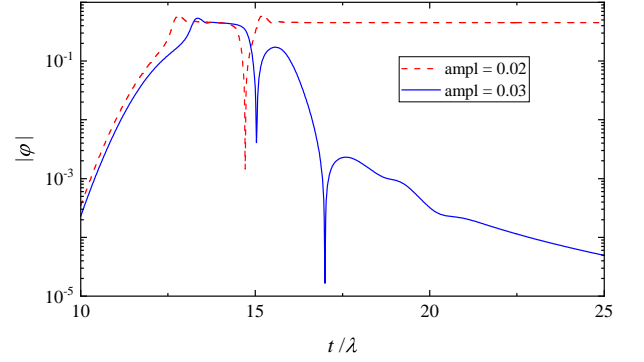


FIG. 5. The time evolution of the scalar field on the background of a Schwarzschild black hole with mass  $M/\lambda = 0.03$  and  $\beta = 500$ . The initial data is a Gauss pulse with amplitudes 0.03 and 0.02, dispersion  $\sigma/\lambda = 1$ , located at coordinate distance  $x/\lambda = 12$ . The used coupling function is  $f_2(\varphi)$ .

with

$$\Psi_r = \lambda^2 \frac{df(\varphi)}{d\varphi} \frac{d\varphi}{dr}. \quad (\text{A12})$$

In order to obtain black hole solutions the following conditions should be imposed coming from the requirements for asymptotic flatness at infinity and the regularity at the black hole horizon  $r = r_H$ :

$$\Phi|_{r \rightarrow \infty} \rightarrow 0, \quad \Lambda|_{r \rightarrow \infty} \rightarrow 0, \quad \varphi|_{r \rightarrow \infty} \rightarrow 0, \quad (\text{A13})$$

$$e^{2\Phi}|_{r \rightarrow r_H} \rightarrow 0, \quad e^{-2\Lambda}|_{r \rightarrow r_H} \rightarrow 0. \quad (\text{A14})$$

The regularity of the scalar field and its first and second derivatives on the black hole horizon leads to an additional condition for the existence of black hole solutions

$$\begin{aligned} \left( \frac{d\varphi}{dr} \right)_H &= \frac{r_H}{4\lambda^2 \frac{df}{d\varphi}(\varphi_H)} \times \\ &\times \left[ -1 + \sqrt{1 - \frac{24\lambda^4}{r_H^4} \left( \frac{df}{d\varphi}(\varphi_H) \right)^2} \right] \end{aligned} \quad (\text{A15})$$

Clearly, solutions can exist only in case the expression inside the square root is positive. For black holes with nontrivial scalar field this condition can be easily violated, though, and it limits (sometimes severely) the domain of existence of scalarized solutions [3].

## Appendix B: Numerical results for the second coupling function $f_2(\varphi)$

### 1. Dynamics with $f_2(\varphi)$

It is clear that the condition for the existence of scalarized phases (2) can be satisfied also for higher powers of

$\varphi$ . In the present paper we are focusing on  $Z_2$  symmetric theories and that is why the next possible choice is to consider coupling function of the type  $f_2(\varphi)$  defined in eq. (3).

The time evolution of scalar field on the Schwarzschild background is shown in Fig. 5 for two different amplitudes of the initial perturbation close to the threshold for the development of a nonlinear instability. As one can see, for smaller amplitude the scalar field perturbation decays exponentially and the quasinormal modes of the Schwarzschild black hole within sGB gravity are observed. A slight increase of the amplitude, though, leads to the formation of a stable equilibrium scalar field configuration at later times.

## 2. Scalarized phases with $f_2(\varphi)$

Having demonstrated that scalarized phases can be indeed dynamically formed for large enough amplitude of the initial perturbation, here we will discuss the complete spectrum of scalarized phase solutions for the coupling  $f_2(\varphi)$  obtained after solving the reduced field equations (A8)–(A11). The scalar field on the horizon, the horizon radius and the scalar charge as a function of mass are plotted in Fig. 6 for several values of  $\beta$ . The minimum  $\beta = 460$  plotted in the figure is very close to the threshold where the scalarized phases disappear. With the increase of  $\beta$  we have three distinct cases similar to the  $f_1(\varphi)$  case:

- For smaller  $\beta$  three branches of solutions exist – two with higher mass spanning a limited range of masses (and not reaching the  $M = 0$  limit), and one branch appearing at relatively low masses. Only the high-mass branch depicted with solid line is potentially stable.
- For intermediate  $\beta$  a similar picture is observed with the difference that the potentially stable branch (depicted with solid line) actually reaches the  $M = 0$  limit.
- For large enough  $\beta$  only two branches of solutions exist starting from the zero mass limit and merging again at some finite  $M/\lambda$ .

The main difference with the results for  $f_1(\varphi)$  is on quantitative level. Scalarized phases appear for

much smaller masses (normalized with respect to  $\lambda$ ) and larger values of  $\beta$ . The maximum differences with Schwarzschild is smaller compared to the  $f_1(\varphi)$  coupling judging from the middle panels in Figs. 3 and 6. Again, even though the differences between some of the

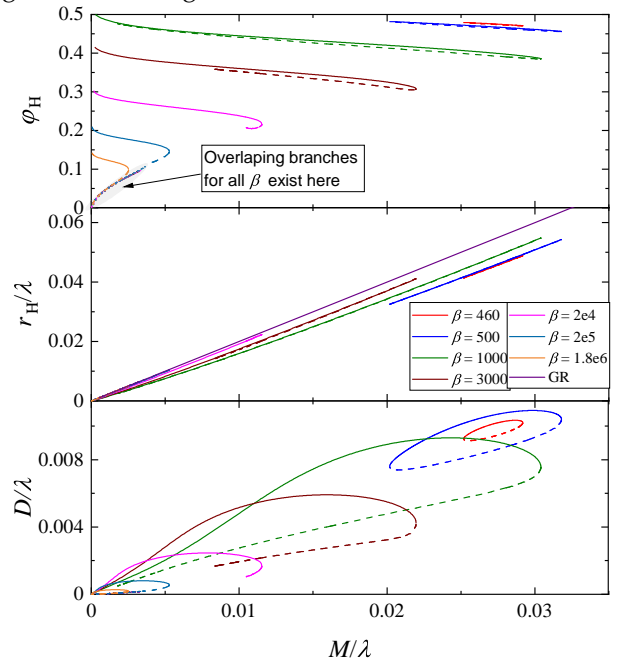


FIG. 6. The scalar field at the horizon (top panel), the mass (middle panel) and the scalar charge (bottom panel) as functions of the black hole mass for the  $f_2(\varphi)$  coupling.

branches (for a fixed  $\beta$ ) look very small if one focuses for example on the behavior of the scalar field at the horizon or the black hole horizon radius, a clear distinction between the scalarized phases is observed in terms of the scalar charge.

The nonlinear simulations show that the only stable branch is the one depicted with a solid line in Fig. 6. In addition, this is the scalarized phase with the highest entropy that is another argument in favor of its stability. Similar to the previous section, for large values of  $\beta$  a small part of the stable hairy black hole branch (close to the maximum mass) can have entropy smaller than the Schwarzschild one but this is quickly reversed with the decrease of the black hole mass. For smaller  $\beta$  the scalarized phase has always larger entropy with respect to Schwarzschild.